RSC Advances

This is an *Accepted Manuscript*, which has been through the Royal Society of Chemistry peer review process and has been accepted for publication.

Accepted Manuscripts are published online shortly after acceptance, before technical editing, formatting and proof reading. Using this free service, authors can make their results available to the community, in citable form, before we publish the edited article. This *Accepted Manuscript* will be replaced by the edited, formatted and paginated article as soon as this is available.

You can find more information about *Accepted Manuscripts* in the Information for Authors.

Please note that technical editing may introduce minor changes to the text and/or graphics, which may alter content. The journal's standard Terms & Conditions and the Ethical guidelines still apply. In no event shall the Royal Society of Chemistry be held responsible for any errors or omissions in this *Accepted Manuscript* or any consequences arising from the use of any information it contains.

ROYAL SOCIETY OF CHEMISTRY

www.rsc.org/advances

Nanoscale surface conductivity analysis of plasma sputtered carbon thin films

Amjed Javid[1,2], Manish Kumar[1], Jeon Geon Han[1,3*]

[1]Center for Advanced Plasma Surface Technology (CAPST), NU-SKKU Joint Institute for Plasma Nano-Materials (IPNM), Advanced Materials Science and Engineering, Sungkyunkwan University, Suwon, 440-746, Korea.

[2]Department of Textile Processing, National Textile University, Faisalabad-37610, Pakistan.

[3]Department of Industrial Engineering, Faculty of Engineering, Chiang Mai University, Chiang Mai-50200, Thailand.

*Corresponding author: Prof. Jeon Geon Han, email: hanjg@skku.edu

RSC Advances Accepted Manuscript

Abstract

Understanding of surface conductivity at nanoscale is very important for surface activities e.g. bio-activity and electronic transportations. In this work, the co-relation of surface properties to surface conductivity has been investigated in carbon films prepared by plasma sputtering. Field Emission Scanning Electron Microscopy (FE-SEM) study provided the evidence of film growth in the form of the nano-domains (NDs). The conductive atomic force microscopy (C-AFM) was used to explore the influence of growth conditions on the local current flow in carbon thin films through the induced current variation across the NDs. It is found that the growth regime of the ND has a close relation to the power density and the working pressure. The flow of current across the internal area of the ND surface is lower than the boundaries due to the difference of conjugation in sp^2 hybridized carbon atoms. The mean current flow through the films as measured by C-AFM is in accordance with the resistivity of the films observed by Van der Pauw method.

Keywords: carbon films, conductive atomic force microscopy, conjugation, electrical resistivity, sp^2 hybridization

RSC Advances Accepted Manuscript

1. Introduction

Carbon films has stimulated and diverted the attention of researchers because of numerous applications such as photovolataic devices,[1] corrosion inhibition, wear resistant[2] and thermal conductive coatings,[3] chemically inert materials,[4] electroanalysis and sensing devices[5] and regenerative medicine.[6] The efforts, regarding use of carbon films in biotechnology, can be attributed to its excellent ability to be inert, biocompatible and bioactive with the host.[7] The key properties of carbon and other biomaterials, necessary for its interaction with the living organisms, include surface chemistry, topography, wetability and electrical resistivity.[8-9] Since, physicochemical surface properties of the materials play key role referring to their interaction with the living organisms,[10] it is of vital importance to address the co-relation between these characteristics and cellular response. Many researchers have reported the influence of surface chemical functionalities,[11] surface roughness[12] and surface energy[13] of biomaterials on the cell adhesion, but only a few studies are available regarding electrical resistivity/conductivity[9,14] in which standard electrical measurement techniques (Hall measurement, 4-point probe method) are used to study the electrical properties of thin films. Arena *et al*. studied the electronic properties (density of states, band gap, shifting of the Fermi level) of amorphous carbon films uning scanning tunneling microscopy.[15] Kim *et al.* reported the enhancement of cell growth on decreasing the resistivity of carbon films.[9] Choi *et al.* observed the co-relation between conductivity of ZnO thin films and SF295 cell morphogenesis and proliferation.[14] Particularly, the studies regarding surface electrical characterization on nanoscale are lacking and there is need to address the phenomenon of nano-scale conductivity variation on film surface to better understand the co-relation between surface conductivity variation and cellular response.

Atomic force microscopy (AFM) is a non-destructive technique to characterize surface

RSC Advances Accepted Manuscript

topography, adhesion, grain size and some other properties on a scale from nanometers to few micrometers.[16,17] Y. F. Dufrêne reported the use of AFM in multi-parametric analysis of microbial cell surfaces, giving deep insight into structure-function relationships.[18] The C-AFM is very promising technique to investigate structural characteristics and conductivity of materials.[19-21] Jiang *et al.* reported the failure analysis on nanometer scale on integrated circuits using C-AFM.[22] In the semiconductor industry, the use of C-AFM is very helpful to explore the electrical and structural characteristics of ErAs nanoparticles incorporated in GaAs.[19] Dai *et al.* explored the structural imperfections and their effect on the conductivity of individual carbon nanotubes via C-AFM.[23] The high spatial resolution measurements, achieved by C-AFM, over other electrical characterizations, is the main reason for motivation and initiation of this research work.

In the present research work, deposition of carbon films is carried out by varying process conditions (power density and pressure) to elucidate their effect on the surface structure and surface conductivity. FE-SEM provides the information about morphological features of the film. The C-AFM provided the deep insight into electrical properties on nanoscale of the carbon film surface. The resistivity was also measured to investigate the overall electrical behavior of films.

2. Experimental

Carbon films, having 200 nm thickness, were deposited on silicon wafer substrates (1 cm × 1 cm) using facing target magnetron sputtering. Prior to deposition, the silicon wafers were cleaned ultrasonically with acetone followed by ethanol each for 15 min. The process chamber was evacuated to 1×10^{-5} Torr base pressure by a rotary pump in conjunction with turbo-molecular pump. Argon gas was used to initiate the sputtering process. A pulse DC (150 kHz, 2.9 μsec) power was supplied to the facing electrodes each having 4 inch graphite

RSC Advances Accepted Manuscript

(99.99 %) target. The films were deposited by varying the power density (4 to 20 W/cm^2) and working pressure (2.5 to 8.5 mTorr).

The films thickness was analyzed through surface profiler (KLA-Tencor, Alpha-Step IQ). The surface conductivity and topography were measured using AFM (NX-10, Park Systems) in contact mode. The silicon probe tip, coated with Cr/Pt conductive coatings, was used to investigate the nanoscale conductivity variation on the surface of deposited films. A positive bias (5 V) was applied across the film and tip of the cantilever. Both the topography and current images were recorded by moving the cantilever across an area of 1μm ×1μm with 256 × 256 data points. An electric current amplifier was used to measure the current flow on the surface of the film.

The electrical resistivity of films was measured by Van der Pauw method (4-point probe). The surface morphological observations were carried out through FESEM technique (FE-SEM, JEOL JSM-6500F).

3. Results and discussion

The FE-SEM images of the carbon films prepared with different power density and working pressure are shown, as (a) 10 W/cm^2, (b) 20 W/cm^2 (at constant 4.5 mTorr pressure) and (c) 2.5 mTorr, (d) 8.5 mTorr (at fixed 20 W/cm^2 power density), in Fig. 1. The top view clearly depicts the formation of ND on the surface during the film deposition. The cross-sectional images of films (inset) show the columnar structure with small channels corresponding to spacing between NDs. It is observed that the spacing between the columns is higher for 10 W/cm^2 as compared to 20 W/cm^2 power density. On the other hand, the less openings are observed for 2.5 mTorr rather than 8.5 mTorr pressure. It shows that the compact structures are grown at higher power density and lower pressure due to bombardment of energetic ions on the film surface.

RSC Advances Accepted Manuscript

The height images are obtained, without applying bias voltage to AFM cantilever, to investigate the surface physical features. In Fig.2, the (a), (b) and (c) corresponds to films prepared at 10 W/cm^2, 15 W/cm^2 and 20 W/cm^2 power density (at fixed 4.5 mTorr pressure) respectively while the (d), (e) and (f) represent the films deposited at 2.5 mTorr, 6.5mTorr and 8.5 mTorr pressure (at fixed 20 W/cm^2 power density). Uniform and smooth films are observed with little variation in surface roughness. The RMS roughness changes in the narrow range of 1.52 nm to 1.82 nm, for all values of power density (5 to 20 W/cm^2) and working pressure (2.5 to 8.5 mTorr). The variation is not significant which depicts that the film surface is smooth and uniform.

The histograms of height distribution have been plotted as a function of power density and pressure and are shown as (a) and (b) respectively in Fig. 2. The 0 nm represents the mean position about which the pixels are distributed. The scanning is carried out on an area of 1 μm × 1 μm having 256 × 256 pixels. Interestingly, the data points for pixel counts are concentrated about the mean position with little variation in distribution range for all values of power density and pressure. Very few pixels are in the wider range which represent the external points of peaks and valleys. Due to this small variation in distribution range, the span of RMS roughness is narrow (1.56 to 1.80 nm). Furthermore, the sharpness of pixel distribution curves increases on increasing the power density and decreasing the pressure. This can be correlated to the accumulation behavoiur of surface NDs. Both at higher power density and lower pressure, the NDs are packed relatively in compact manner and showing the more pixels about 0 nm.

The film growth phenomenon is closely related to the plasma process parameters and can be controlled by controlling the plasma conditions. The plasma process conditions are varied by changing the power density and working pressure. On increasing the power density, the gaps

RSC Advances Accepted Manuscript

between the ND become narrower, making a structure in which these are tightly packed. At elevated power, the energetic ions, approaching the growing films, directly influence the film growth phenomenon and produce a structure with more compact and tightly packed NDs with minimal spacing. However, the increase in working pressure gives the structures of lower compactness with relatively wider gaps between NDs. At high pressure, the electron temperature decreases and the impact of bombardment of the excited species on the growing film is less effective and the resulting films are grown with the structures of lower compactness. So, the film growth can be well controlled by controlling the plasma conditions to tailor a structure of desired properties. These results are supported by the SEM cross-sectional images where the openings between columnar structures illustrate the film growth behaviour.

The electrical resistivity of the carbon film is observed as function of power density and pressure. The results are shown in Fig. 3. The observations depict that there is significant effect of power density and pressure on resistivity of carbon films. A reduction in resistivity of the order of 10^3 is observed on increasing the power density from 5 to 20 W/cm^2. However, an increasing trend in resistivity, with the order of 10^2, is observed on changing pressure from 2.5 to 8.5 mTorr. The resistivity of carbon films mainly depends upon the amount of sp^2 hybridized carbon atoms which are responsible to generate conjugation due to delocalization of π electrons. The increase in power density enhances the electron temperature [9] which gives rise to the formation of more graphitic nano-clusters of sp^2 phase. This phenomenon leads to increase the number of π states causing reduction in resistivity of the films. Similarly, in case of increasing pressure the electron temperature decreases[24] and an increase in resistivity is observed due to reduction of sp^2 phases.

The current images of carbon films are obtained by scanning over 1 μm × 1 μm through

RSC Advances Accepted Manuscript

conductive tip of AFM. In Fig. 4, the images of carbon films, prepared as function of power density, are shown as (a), (b), (c) and (d), corresponding to 5 W/cm^2, 10 W/cm^2, 15 W/cm^2 and 20 W/cm^2 (at fixed 4.5 mTorr pressure) respectively. Similarly, the images of the films, deposited as function of pressure, are shown as (e), (f) and (g), representing the 2.5 mTorr, 6.5 mTorr and 8.5 mTorr pressure (at fixed 20 W/cm^2 power density) respectively in Fig. 4. The film growth process is carried out, in such a way to generate two types of contrast regions in nanometer scale. These regions, having dissimilar reflections, can be seen clearly in the Fig.4. The dark regions represent the areas where the carbon species are joined together to form ND. The dark areas have relatively lower current flow as compared to the bright channels. The bright areas represent the ND boundaries and exhibit the relatively higher current flow zones. The difference of conductivity between the internal areas and boundaries of NDs is attributed to difference of π electron density. This concept is explained by drawing a schematic diagram, representing the variation of π electron density on film surface and is shown as (h) in Fig. 4. The grey spheres illustrate the NDs and blue dots represent the π electrons (responsible for conductivity). The difference in conductivity is further explained by selecting the two adjacent NDs (white dotted squares), and plotting the current flow against the distance for 2.5 and 8.5 mTorr pressure at fixed power density (20 W/cm^2), and are shows as (i) and (j) respectively. Both the graphs show wavy lines, each having single large peak corresponding to higher current flow across the area between NDs (bright region). The wavy lines (without large peaks) represent the internal area of ND surface (dark region).

The line profile of current on the surface of the film is observed as function of pressure and shown, as (a) and (b) referring to 2.5 mTorr and 8.5 mTorr (at fixed 20 W/cm^{2}power density) respectively, in Fig. 5. A variation in current is observed as the tip of C-AFM passes across the surface of carbon film (1 μm length). This variation is centered about a mean value and

RSC Advances Accepted Manuscript

can be divided into lower and higher current values, corresponding to the contrast regions (dark and bright) as mentioned earlier. The lower peaks correspond to the centers of the NDs surface areas. These peaks are less sharp, which is due to the less variation in conductivity at central areas. As the tip moves towards the boundaries, then near the edges of these NDs, the variation in conductivity starts increasing and sharp peaks appear. The sharp peaks, above the mean line, show the rapid change in conductivity and also exhibit the smaller areas between NDs.

The mean current flow across the film surface as measured by C-AFM varies between the nA to μA. A directly proportional relationship exists between the amount of current flow and power density. However, the current flow decreases upon increasing pressure (Fig. 6). The maximum current flow value (0.426 μA) is observed for 20 W/cm^2 and 2.5 mTorr (the highest power density and the lowest pressure in this study). The dependence of surface conductivity of carbons films, upon power density and pressure, is attributed to the number of sp^2 hybridized carbon atoms and is in accordance with the 4-point probe observations.

The diamond like carbon films are mixtures of sp^2 and sp^3 hybridized carbon atoms. The electrical conductivity of carbon films as reported by many researchers[9,25,26] depends upon the amount of sp^2 bonds. The sp^2 hybridization process, in materials fabrication, is originated from the combination of 1s and two p (p_x and p_y) orbitals. The p_z orbital does not take part in hybridization and is perpendicular to the plane of hybrid sp^2 orbitals. The additional p_z orbitals of adjacent carbon atoms share their electron to make π bonds. The electrons of these bonds are known as π electrons.[27] The π electrons are not tightly bound and have some freedom to move across the participating atoms and give rise to phenomenon of delocalization. The delocalized π electrons cannot exist independently. They are influenced by the adjacent π bonds to form benzene like conjugated system. So, each π bond has

RSC Advances Accepted Manuscript

contributions due to adjacent π bonds and this provides long-range polarizabilities due to long-range forces.[28] Here, it should be noted that all the samples were kept in identical conditions (in isolated vacuum boxes) between the sample preparation and surface conductivity testing duration. The reproducibility of C-AFM measurements were checked in back and forth mode and found satisfactory to distinguish the noise (as background) and signal (as information) level. The effect of atmospheric exposure in properties of carbon films e.g. surface energy, wettability, resistivity, and sp^2 bonding, is extensively investigated and submitted elsewhere.

The sp^2 hybridized carbon atoms, forming π bonds, are distributed on the surface of carbon films. The distribution of the sp^2 hybridized carbon atoms, on the surface of the NDs, occurs in a narrow range of variation. This is evidenced by the mean current flow data. A little variation in current flow is observed upon moving the conductive tip on the ND surface. A higher current flow, observed at the boundaries as compared to the internal areas of the NDs, exhibits that an enhancement in density of charge transport species occurs at the boundaries. The higher current flow at the boundaries is attributed to the difference of conjugation due to π electrons of sp^2 hybridized carbon atoms at the internal areas and boundaries of NDs. At the boundaries, the conjugation is higher due to higher electron density and additional conjugations are contributed from the sp^2 hybridized carbon atoms of the neighbouring NDs. So, there is relatively higher density of π electrons at the boundaries to enhance the conductivity. At the ND boundaries, a nano-interface exists where a rapid change in current flow gives the evidences about the existence of enhanced conjugation.

4. Conclusions

The conductive carbon film with smooth and homogeneous surface is prepared using magnetron sputtering. The surface morphology ehhibits the nano-damins on the surface of

RSC Advances Accepted Manuscript

carbon film. The C-AFM is used to explore the conductivity variation on the film surface. Two types of the regions, bright and dark corresponding to higher and lower current flow respectively, are observed on the surface. The phenomenon of conductivity variation, on the internal area of NDs and at the boundaries, is generated due to the difference of conjugation contributed by the π states of sp^2 hybridized carbon atoms.

Acknowledgements

This work is supported by Leading Foreign Research Institute Recruitment Program through the National Research Foundation of Korea funded by the Ministry of Science, the ICT and Future Planning (MSIP) (2011-0031643), Global Development Research Center, and Korea Institute for the Advancement of Technology (KIAT) funded by the Ministry of Trade, Industry & Energy (MOTIE) (N0000590).

References

1 T. Cui, R. Lv, Z. H. Huang, X. Gan, K. Wang, D. Wu, H. Zhuac and F. Kang, *RSC Adv.*, 2013, **3**, 22295

2 T. Falacade, T. Eduardo, O. Gomes, A. Luis, M. Vargas, R. Hubler, I. Lourdes, and C. De Fraga, *Appl. Surf. Sci.*, 2012, **263**, 18.

3 M. Shakerzadeh, M. K. Samani, N. Khosravian, E. H. T. Teo, M. Bosman and B. K. Tay, Carbon, 2012, **50**, 1428.

4 J. Xue, C. Henry, J. Lee and B. D. Vogt, *RSC Adv.*, 2014, **4**, 3675.

5 L. B. Sheridan, D. K. Hensley, N. V. Lavrik, S. C. Smith, V. Schwartz, C. Liang, Z. Wu, H. M. Meyer, and A. J. Rondinone, *J. Electrochem. Soc.*, 2014, **161**, H-558.

6 D. A. Cantu, P. Hematti, W. J. Kao, *Stem Cells Transl. Med.*, 2012, **1**, 740.

7 Y. Tzeng, S. Yeh, W. C. Fang and Y. Chu, *Sci. Rep.*, 2014, **4**, 4531.

8 K. Anselme, L. Ploux and A. Ponche, *J. Adhes. Sci. Technol.*, 2010, **24**, 831.

RSC Advances Accepted Manuscript

9 S. I. Kim, B. B. Sahu, S. E. Kim, A. Ali, E. H. Choi and J. G. Han, *J. Mater. Chem. B*, 2015, **3**, 3267.

10 V. Peˇs´akov´a, D. Kubies, H. Hulejov´a and L. Himmlov´a, *J. Mater. Sci. Mater. Med*. 2007, **18**, 465.

11 X. Liu, Q. Feng, A. Bachhuka, and K. Vasilev, *ACS Appl. Mater. Interfaces*, 2014, **6**, 9733.

12 E. Biazar, M. Heidari, A. Asefnezhad and N. Montazer, Int. J. Nanomed., 2011, **6**, 631.

13 H. C. Lai, L. F. Zhuang, X. Liu, M. Wieland, Z.-Y. Zhang and Z. Y. Zhang, *J. Biomed. Mater. Res. Part A*, 2010, **93**, 289.

14 W. Choi, J. Jung, S. Lee, Y. J. Chung, C. –S. Yang, Y. K. Lee, Y. –S. Lee, J. K. Park, H. W. Ko and J.-O. Lee, *Sci.Rep*., 2015, **5**, 9974.

15 C. Arena, B. Kleinsorge, J. Robertson, W. I. Milne and M. E. Welland, J. Appl. Phys. 1999, 85, 1609.

16 S. N. Magonov and D. H. Reneker, *Annu. Rev. Mater. Sci*., 1997, **27**, 175.

17 N. E. Gorji, U. Reggiani, and L. Sandrolini, Int. J. Photoenergy, 2015.

18 Y. F. Dufrêne, *mBio*., 2014, **5**.e01363-14.

19 K. W. Park, V. D. Dasika, H. P. Nair, A. M. Crook, S. R. Bank, and E. T. Yu, *Appl. Phys. Lett*., 2012, **100**, 233117

20 S. Kwon, H. J. Chung, S. Seoc and J. Y. Park, *Surf. Interface Anal*., 2012, **44**, 768.

21 R. Hiesgen, T. Morawietz, M. Handl, M. Corasaniti, and K. A. Friedrich, *J. Electrochem.Soc*., 2014, **161**, F1214.

22 Y. Jiang, L. L. Lai, J. J. Zhou, *Microelectron. Reliab*., 2012, **52**, 159.

23 H. Dai, E. W. Wong, C. M. Lieber, *Science*, 1996, **272**, 523.

24 S. I. Kim, B. B. Sahu, B. M. Weon, J. G. Han, J. Koskinen and S. Franssila, *Jpn. J. Appl. Phys*., 2015, **54**, 010304.

RSC Advances Accepted Manuscript

25 R. Li, K. Parvez, F. Hinkel, X. Feng, and K. Mullen, *Angew. Chem. Int. Ed*. 2013, **52**, 5533.

26 K. Torbensen, J. Iruthayaraj, M. Ceccato, M. Kongsfelt, T. Breitenbach, S. U. Pedersen and K. Daasbjerg, *J. Mater. Chem*, 2012, **22**, 18172.

27 J. Robertson, *Mater. Sci. Eng*., 2002, **37**, 129.

28 A. C. Ferrari and J. Robertson, Phys. Rev. B, 2000, **61**. 14095

Figure captions

Figure 1. FESEM images of carbon films deposited at various, power density (a) 10 W/cm^2, (b) 20 W/cm^2 (at fixed 4.5 mTorr pressure) and pressure (c) 2.5 mTorr, (d) 8.5 mTorr (at fixed 20 W/cm^2 power density). The images have both top and cross-sectional (inset) view with magnification × 100,000.

Figure 2. Height images of carbon films deposited with varying, power density (a) 10 W/cm^2, (b) 15 W/cm^2, (c) 20 W/cm^2 (at fixed 4.5 mTorr pressure) and pressure (d) 2.5 mTorr, (e) 6.5 mTorr, (f) 8.5 mTorr (at fixed 20 W/cm^2 power density). The scale bar is 1 μm × 1 μm. Histograms illustrate the height distribution as a function of (g) power density at fixed 4.5 mTorr pressure and (h) pressure at fixed 20 W/cm^2 power density.

Figure 3. Electrical resistivity of carbon films as a function of power density at fixed pressure (4.5 mTorr) and as a function of pressure at fixed power density (20 W/cm^2).

Figure 4. The current images of carbon films deposited by varying power density (a) 5 W/cm^2, (b) 10 W/cm^2, (c) 15 W/cm^2, (d) 20 W/cm^2 (at fixed 4.5 mTorr pressure) and by varying pressure (e) 2.5 mTorr, (f) 6.5 mTorr (g) 8.5 mTorr (at fixed 20 W/cm^2 power density). The scale bar is 1 μm × 1 μm. Schematic diagram of π electron density variation is shown as (h). The grey spheres represent the NDs and blue dots correspond to π electrons. Line profiles of current of selected area (white spheres) represent the films (magnified image) deposited at (i) 2.5 mTorr pressure and (j) 8.5 mTorr pressure at fixed 20 W/cm^2 power density.

RSC Advances Accepted Manuscript

Figure 5. The line profile of current variation on the surface of carbon film deposited at 20 W/cm^2 with varying pressure (a) 2.5 mTorr, (b) 8.5 mTorr. The sharp peaks on the higher side depict the ND boundaries while the blunt peaks at lower side represent the internal areas of NDs surface.

Figure 6. Mean current variation probed through conductive tip of AFM as a function of, power density (at fixed 4.5 mTorr pressure) and pressure (at fixed 20 W/cm^2 power density).

Figure 1

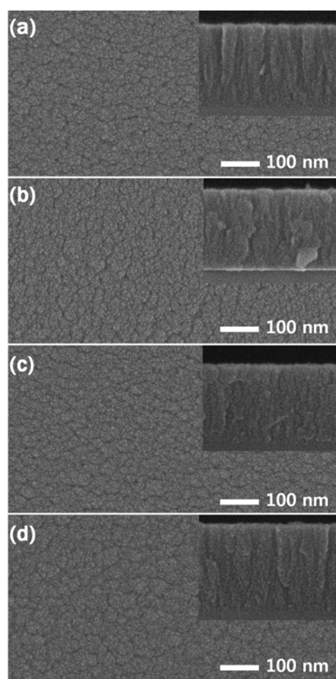

RSC Advances Accepted Manuscript

Figure 2

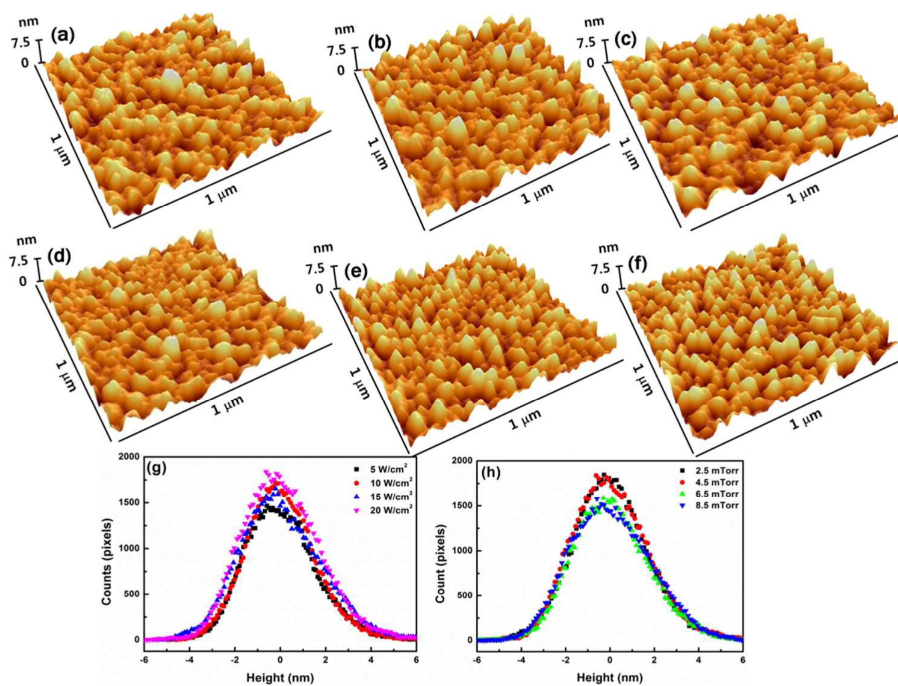

RSC Advances Accepted Manuscript

Figure 3

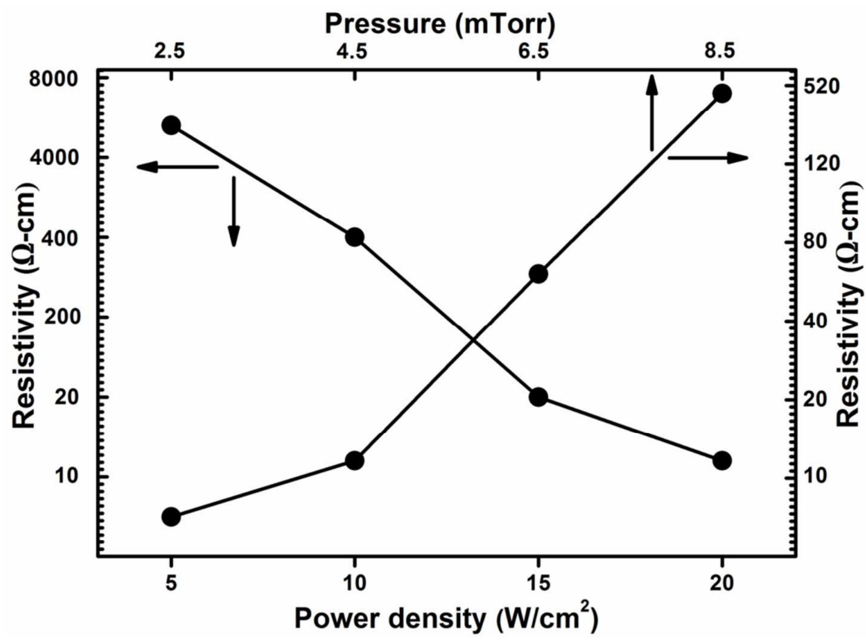

RSC Advances Accepted Manuscript

Figure 4

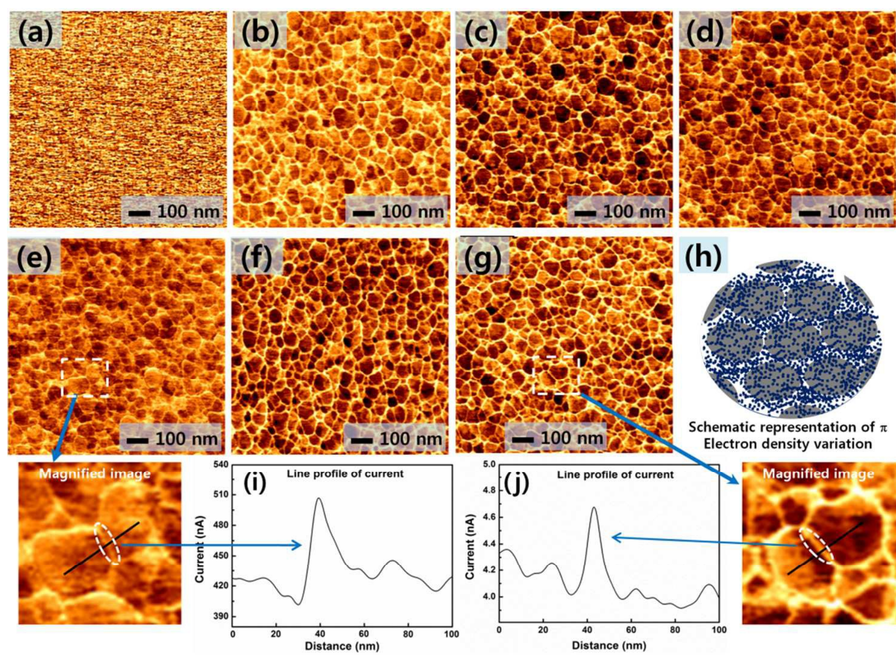

RSC Advances Accepted Manuscript

Figure 5

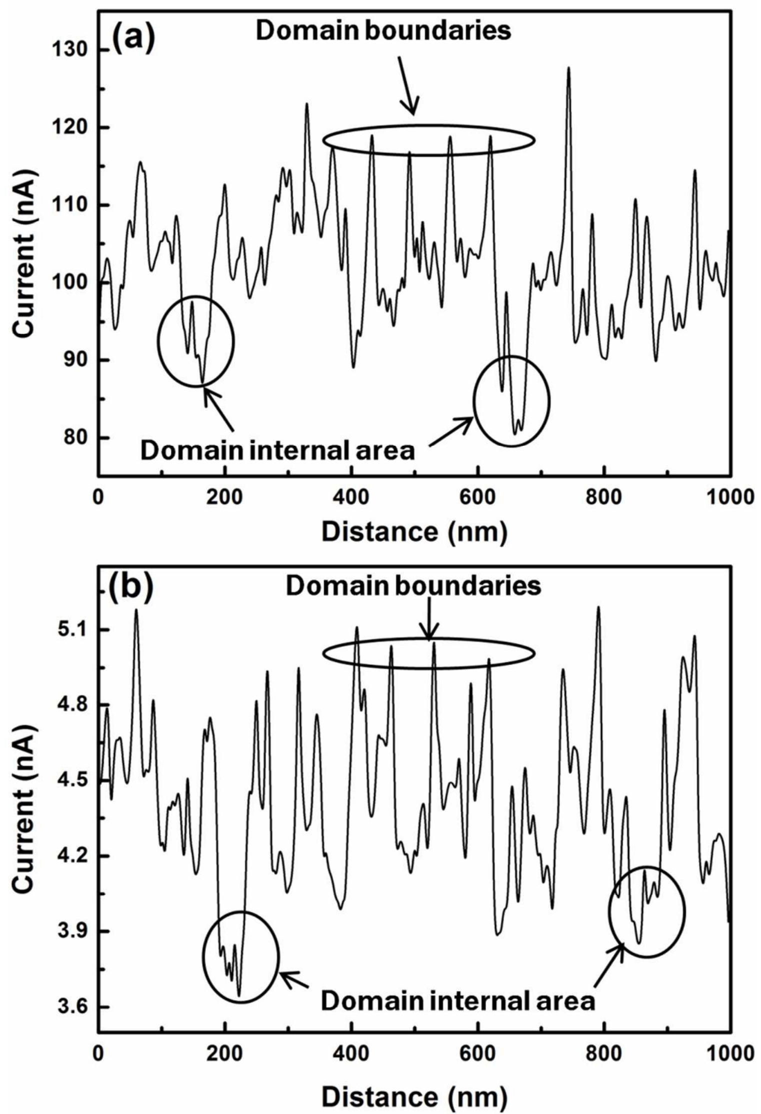

RSC Advances Accepted Manuscript

Figure 6

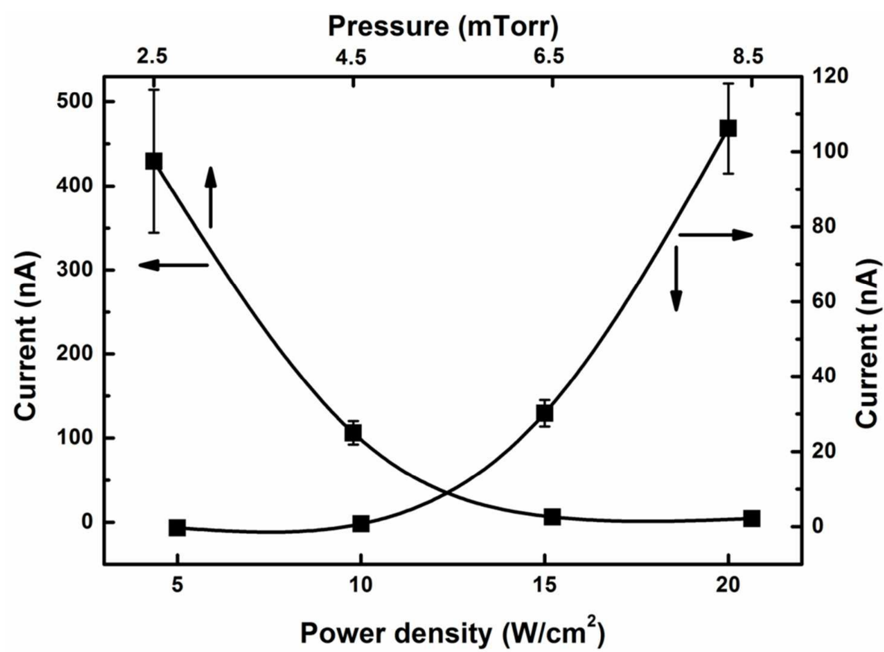

RSC Advances Accepted Manuscript